Sequential retrieval of non-random patterns in a neural network

1990 J. Phys. A: Math. Gen. 23 4627

(http://iopscience.iop.org/0305-4470/23/20/024)

J. Phys. A: Math. Gen. 23 (1990) 4627-4641. Printed in the UK

Sequential retrieval of non-random patterns in a neural network

Tota Nakamura and Hidetoshi Nishimori

Department of Physics, Tokyo Institute of Technology, Oh-okayama, Meguro-ku, Tokyo 152, Japan

Received 14 June 1990

Abstract. A neural network capable of retrieval of sequential patterns is analysed. We treat the network proposed by Buhmann and Schulten. Although they concluded that the thermal noise induces retrieval of sequential patterns, we show that the network has limit cycle solutions even at zero temperature. Behaviour of the network at high temperatures is also analysed. The transition temperatures between a high-temperature fixed point phase and a limit cycle phase are calculated numerically to draw a phase diagram. The characteristic features of the phase diagram are discussed. The reentrant transition temperatures between the limit cycle and low-temperature fixed point phases are calculated analytically.

1. Introduction

A neural network with symmetric interactions serves as an associative memory of static patterns. As long as the number of embedded patterns remains small enough as compared with the number of neurons, the network evolves until it eventually reaches the nearest pattern when started from the neighbourhood of one of the embedded patterns. Each retrieved state is regarded as a fixed point of the dynamics of the network. No other types of attractors exist in the symmetric networks.

It is necessary to introduce asymmetry in interactions to construct a dynamical associative memory (or a network which retrieves spatio-temporal sequences). There have been quite a few asymmetric networks proposed for dynamical associative memory. A simple synchronous network has been shown to work as a dynamical associative memory (Amari 1972), but an asynchronous counterpart has been considered to be incapable of retrieval of spatio-temporal sequences (Hopfield 1982). Introduction of delay in signal transmission has been regarded as a key ingredient in constructing a dynamical associative memory in an asynchronous network (Sompolinsky and Kanter 1986). We have shown in a recent paper (Nishimori *et al* 1990) that this is not necessarily the case by explicitly giving the asymmetric interactions with no signal delay causing a sequential retrieval of embedded patterns. A different type of asymmetric network has been proposed by Buhmann and Schulten (1987) who claimed that thermal noise induces transition from a pattern to the next, even in the absence of signal delay. In their network, each neuron has two states, 1 or 0, which corresponds to the state of firing or being at rest. A neuron is assumed to be firing at most in one of the patterns. In other words, there are no common firing regions shared by different patterns. This latter restriction allows us to embed meaningful (non-random) patterns in an orthogonal way which is often essential in an associative memory (see

0305-4470/90/204627+15$03.50

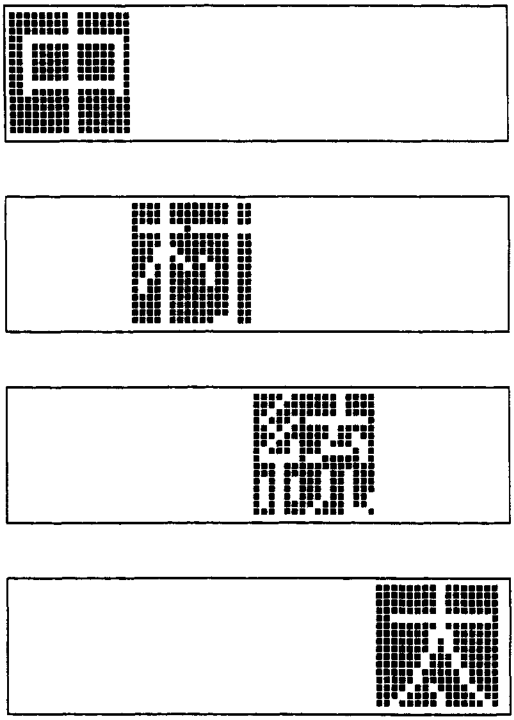

Figure 1. An example of orthogonal embedded patterns meaning the name of one of the authors, 'Naka', 'mura', 'To', 'ta', in Japanese. Black points are firing neurons and others are resting. A firing region of each pattern does not have an overlap with that of others.

figure 1). They have shown that such a network has a limit cycle solution, corresponding to sequential retrieval of patterns, only at finite temperatures. We prove in the present paper that it is possible to construct a similar network even in the absence of thermal noise. We clarify the conditions under which the network has a limit cycle solution. The results of Buhmann and Schulten are included as a special case in our general criterion.

2. Description of the network

We choose the synaptic interaction J_{ij} slightly different from that of Buhmann and Schulten:

$$J_{ij} = \sum_{\mu=1}^{p} (\alpha\varepsilon^{\mu-1}\xi_j^{\mu-1} + \varepsilon^{\mu}\xi_j^{\mu} - \beta\varepsilon^{\mu+1}\xi_j^{\mu+1})\xi_i^{\mu} \tag{2.1}$$

where ξ_i^{ν} assumes 1 if neuron i is firing in the νth pattern and 0 otherwise. The parameter α denotes the strength of an excitatory coupling and β represents that of an inhibitory one. The parameters α and β will be adjusted so that the network has a limit cycle solution. Since the number of firing neurons depends on the pattern, we introduce a normalization constant ε^{μ} defined by

$$\sum_{i=1}^{N} \varepsilon^{\mu}\xi_i^{\mu}\xi_i^{\nu} = \delta_{\mu\nu}. \tag{2.2}$$

Equation (2.1) qualitatively means that a neuron receives excitatory inputs from neurons that are active in the previous pattern, inhibitory inputs from active neurons in the next pattern, and autocorrelated self-retrieving excitatory inputs from active neurons in the present pattern. Apparently the interaction (2.1) is asymmetric, $J_{ij} \neq J_{ji}$, which induces sequential retrievals of embedded patterns $\{\xi_i^\mu\}$. No neuron is allowed to fire in more than one pattern as mentioned before. An example of patterns satisfying this condition is given in figure 1.

The dynamical variable $S_i(t)$, the state of the ith neuron, evolves according to the rule

$$S_i(t+1)=\begin{cases}1 & \text{with probability } f_i(t)\\ 0 & \text{with probability } 1-f_i(t)\end{cases} \tag{2.3}$$

where $f_i(t)=(1+\exp[-(h_i-U)/T])^{-1}$ with $h_i=\Sigma_k J_{ik}S_k(t)$. The parameter U denotes the threshold and T represents the temperature or the noise level. The updating process (2.3) is carried out asynchronously for each neuron.

It is convenient to consider a set of macroscopic variables, or the overlap $\{x^\mu\}$, of the current state with the embedded pattern

$$x^\mu(t)=\sum_{i=1}^{N}\varepsilon^\mu\xi_i^\mu S_i(t). \tag{2.4}$$

Following Buhmann and Schulten, we can derive the evolution equation of the overlap as

$$\dot{x}^\mu=-x^\mu+\frac{1}{1+\exp[-(\Xi^\mu-U)/T]} \tag{2.5}$$

where

$$\Xi^\mu=\alpha x^{\mu-1}+x^\mu-\beta x^{\mu+1}.$$

In the derivation of (2.5) it has been assumed that the number of neurons N tends to infinity. Correspondingly the normalization factors ε^μ are considered to be vanishingly small. The number of firing neurons in a pattern grows indefinitely as the system size tends to infinity. Recall that ε^μ is the reciprocal of the number of firing neurons in the μth pattern (see (2.2)). Since we assume that the number of patterns p remains finite in the thermodynamic limit $N\to\infty$, the number of equations (2.5) of the macrovariables is much smaller than that of the microscopic evolution rule (2.3). We investigate the properties of the solution of (2.5) in the following sections. In section 3 we derive the limit cycle conditions at $T=0$ from the stability analysis of the solution of (2.5). In section 4 we investigate the network at higher temperatures where the network is strongly disturbed by thermal noise. In section 5 we estimate the temperature and parameter region where limit cycle solutions exist by the numerical solution of (2.5) and draw phase diagrams. A part of phase boundary lines can be derived analytically. The last section is devoted to symmary and discussion.

3. Limit cycle conditions at $T=0$

In the absence of the thermal noise, or at $T=0$, (2.5) reduces to

$$\dot{x}^\nu=-x^\nu+\theta(\alpha x^{\nu-1}+x^\nu-\beta x^{\nu+1}-U) \qquad (\nu=1,\ldots,p) \tag{3.1}$$

where

$$\theta(x)=\begin{cases}1 & \text{for } x>0\\ 0 & \text{for } x<0.\end{cases} \tag{3.2}$$

We impose a periodic boundary condition $x^{p+1}=x^1$. Equation (3.1) means that x^ν approaches 1 or 0 depending on the sign of $\alpha x^{\nu-1}+x^\nu-\beta x^{\nu+1}-U$. Thus the second term on the right-hand side (RHS) of (3.1) gives the νth component of the overlap vector which the network tries to approach in the p-dimensional phase space $\boldsymbol{x}=(x^1,\ldots,x^p)$. This phase space is divided into 2^p subdomains by the set of $(p-1)$-dimensional hyperplanes $\alpha x^{\nu-1}+x^\nu-\beta x^{\nu+1}-U=0$ $(\nu=1,\ldots,p)$ since each plane divides the space into two regions. As the expression $\alpha x^{\nu-1}+x^\nu-\beta x^{\nu+1}-U$ has a definite sign in each of the 2^p subdomains, x^ν tends monotonically to the target point 1 or 0. Accordingly the vector $\boldsymbol{x}$ monotonically approaches a target point whose component is 1 or 0, as long as $\boldsymbol{x}$ stays within the subdomain. There are two possibilities concerning the relative locations of the target point vector and the subdomains. If the target point vector lies within its corresponding subdomain, the vector $\boldsymbol{x}$ reaches the target point. This implies that the network stays stuck to the stable fixed point. On the other hand, for a limit cycle solution to exist, it is sufficient to have no target point in its corresponding subdomain in order that $\boldsymbol{x}$ does not reach any of the stable target points. However, this sufficient condition is not actually satisfied. For example, $(0,0,\ldots,0)$ is always stable (that is, this is the target point of a subdomain in the neighbourhood of this point) even when the limit cycle exists. This fact can be verified by substituting 0 into all x^ν's in the argument of θ in (3.1). For our purpose of dynamical associative memory, this trivial fixed point $(0,0,\ldots 0)$ does not play a role; we have only to consider a limit cycle solution starting from the retrieval of the first pattern $(1,0,\ldots,0)$, evolving to the second $(0,1,\ldots,0)$ and ending up in the last pattern $(0,0,\ldots,1)$ to return to the original one $(1,0,\ldots,0)$. The network evolves in the same manner as above afterwards. We thus discuss the evolution from $(1,0,\ldots,0)$ to $(0,1,\ldots,0)$. The other part of the limit cycle solution automatically emerges because the system is constructed symmetric under the cyclic exchange of the pattern index. Therefore we restrict ourselves to the successive two components of vector $\boldsymbol{x}$ and derive the condition for the system to move from $(1,0)$ to $(0,1)$ on the plane $(x^\nu,x^{\nu+1})$.

The flow equations of x^ν and $x^{\nu+1}$ are

$$\begin{aligned}\dot{x}^\nu&=-x^\nu+\theta(\alpha x^{\nu-1}+x^\nu-\beta x^{\nu+1}-U)\\ \dot{x}^{\nu+1}&=-x^{\nu+1}+\theta(\alpha x^\nu+x^{\nu+1}-\beta x^{\nu+2}-U).\end{aligned}\tag{3.3}$$

There are four subdomains determined by the sign of the arguments of θ. The target point of each subdomain is indicated in figure 2. From this figure one finds the following conditions for a limit cycle solution to exist.

(i) The retrieved state $(1,0)$ should not be in the basin of attraction of $(0,0)$. Otherwise it evolves straight to the trivial state. Since a boundary line intersects the x^ν-axis at $U-\alpha x^{\nu-1}$ as seen in figure 2, the present condition is satisfied if

$$U-\alpha x^{\nu-1}<1.\tag{3.4}$$

(ii) The retrieved state $(1,0)$ should not be stable. That is, the argument of the first θ of (3.3) should not be positive and that of the second should not be negative, when we insert $x^\nu=1$ and $x^{\nu+1}=0$:

$$\alpha x^{\nu-1}+1-U>0\tag{3.5}$$

$$\alpha-\beta x^{\nu+2}-U>0.\tag{3.6}$$

Actually the first relation (3.5) automatically follows from (3.4).

(iii) The simultaneous retrieval state $(1,1)$ of the successive patterns should not be stable. Thus, by inserting $x^\nu=x^{\nu+1}=1$ in the argument of the first θ in (3.3), we

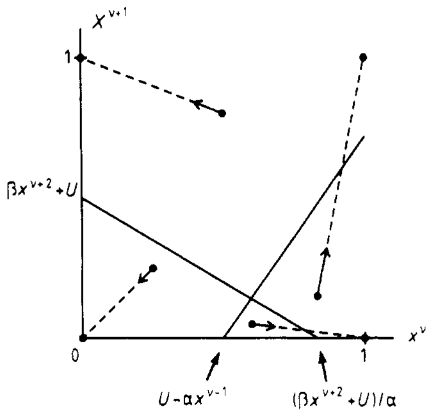

Figure 2. The phase plane $(x^{\nu}, x^{\nu+1})$ is divided into four subdomains by two boundary lines $\alpha x^{\nu-1}+x^{\nu}-\beta x^{\nu+1}-U=0$ and $\alpha x^{\nu}+x^{\nu+1}-\beta x^{\nu+2}-U=0$. Each subdomain is represented by a target point. For example, in the subdomain above both boundary lines, every point moves toward the point $(x^{\nu}, x^{\nu+1})=(0,1)$. This region is represented by the point $(0, 1)$. $\alpha=0.6$, $\beta=0.7$, $U=0.5$.

require

$$\alpha x^{\nu-1}+1-\beta-U<0. \tag{3.7}$$

The argument of the second θ in (3.3) is always positive according to (3.6):

$$\alpha+1-\beta x^{\nu+2}-U>0. \tag{3.8}$$

Equations (3.4), (3.6) and (3.7) are therefore the condition for the limit cycle solution to appear at $T=0$. These inequalities must hold for any value of $x^{\nu-1}$ and $x^{\nu+2}$. When $x^{\nu-1}=x^{\nu+2}=0$, we find

$$1-U>0 \tag{3.9}$$

$$\alpha-U>0 \tag{3.10}$$

$$\beta+U>1. \tag{3.11}$$

Equation (3.4) is satisfied by any value of $x^{\nu-1}$ if satisfied by $x^{\nu-1}=0$. However, (3.6) and (3.7) restrict the values of $x^{\nu-1}$ and $x^{\nu+2}$.

In conclusion, the limit cycle solution can exist even at $T=0$ if the parameters α, β and U satisfy the inequalities (3.9)-(3.11), if the initial condition of $(x^{\nu}, x^{\nu+1})$ lies outside of the basin of attraction of the stable fixed point $(0, 0)$, and if the values of $x^{\nu-1}$ and $x^{\nu+2}$ satisfy (3.6) and (3.7).

Values of α, β and U determine the actual trajectory in the space $(x^{\nu}, x^{\nu+1})$. The turning point where the vector $\boldsymbol{x}$ crosses the boundary line between two sub-domains on the $(x^{\nu}, x^{\nu+1})$ plane is derived in the following. When the components other than x^{ν} and $x^{\nu+1}$ have non-zero value, the phase point stays at $(0, 0)$ on the $(x^{\nu}, x^{\nu+1})$ plane. Then the vector $\boldsymbol{x}$ moves from the point $(0, 0)$ through the x^{ν}-axis to $(U/\alpha, 0)$ beyond which the target point becomes $(1, 1)$ as seen from figure 3. There the vector $\boldsymbol{x}$ turns to move toward $(1, 1)$, but soon it changes the trajectory to the point $(0, 1)$. This turning point is

$$(x^{\nu}, x^{\nu+1})=\left(\frac{\beta-\alpha+U}{\alpha\beta-\alpha+U}\,U, \frac{1-\alpha}{\alpha\beta-\alpha+U}\,U\right) \tag{3.12}$$

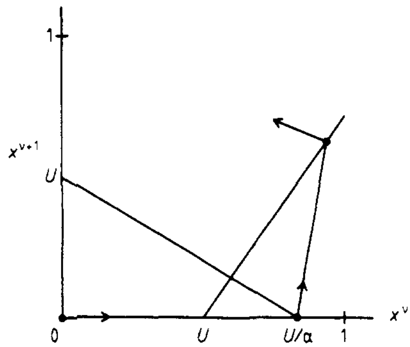

Figure 3. The flow of the vector x projected on the plane $(x^{\nu}, x^{\nu+1})$. As long as both the νth and $(\nu+1)$th components of x do not have values, the phase point stays at $(x^{\nu}, x^{\nu+1}) = (0,0)$ (dotted). Then the νth component gradually grows and the phase point moves toward the point $(1,0)$ until it reaches $(U/\alpha, 0)$ (dotted). There the phase point changes the direction to $(1,1)$. At the point given by (3.12) (dotted), the phase point turns to $(0,1)$. $\alpha=0.6$, $\beta=0.7$, $U=0.5$.

when $x^{\nu+2} = x^{\nu-1} = 0$. The νth component of this point (3.12) is always decreasing with increasing α, β and U. Therefore if α or β is small, the trajectory of the vector x is close to $(1,1)$, which means the network keeps two successive patterns well-retrieved during the transition between the patterns. When U is small, the good retrieval of the pattern is not expected; as U is the threshold, each neuron could be firing randomly. In this case the network does not work as an excellent associative memory. In figure 2 we give an example of the case $\alpha=0.6$, $\beta=0.7$ and $U=0.5$.

4. High-temperature behaviour

At high temperatures the network behaves like a paramagnetic system; each neuron is firing randomly and the activity (the ratio of firing neurons) does not change with time. When we start the network with the initial condition $(1,0,\ldots,0)$, the overlap $\{x^{\nu}\}$, which is generally a function of time, converges to a value determined by temperature and parameters independent of the pattern. As the neurons are firing randomly, this state of constant x^{ν} could be called 'a paramagnetic fixed point' in contrast to 'a retrieval fixed point' such as $(1,0,\ldots,0)$. In this section, we discuss the paramagnetic fixed point as a function of the temperature and the other parameters in the high temperature limit as well as in the neighbourhood of $x^{\nu}=0$ or 1.

4.1. Expansion from the high-temperature limit

The evolution equation of overlaps in the high-temperature limit can be written by the expansion of the exponential function in (2.5) for small $(\Xi^{\nu} - U)/T$

$$\dot{x}^{\nu} = -x^{\nu} + \frac{1}{2} + \frac{\Xi^{\nu} - U}{4T}. \tag{4.1}$$

Let us now introduce the variable δ^{ν} which is the deviation from the fixed point value in the infinite-temperature limit $x^{\nu} = \frac{1}{2}$. Then (4.1) can be written as

$$x^{\nu} = \delta^{\nu} + \tfrac{1}{2} \tag{4.2}$$

$$\dot{\delta}^{\nu} = D_{\nu\mu}\left(\delta^{\mu} + \frac{1}{2}\,\frac{\alpha-\beta-2U+1}{\alpha-\beta-4T+1}\right) \equiv D_{\nu\mu}(\delta^{\mu} - d) \tag{4.3}$$

where

$$D=\frac{1}{4T}\begin{pmatrix} 1-4T & -\beta & & & & \alpha \\ \alpha & 1-4T & -\beta & & & \\ & \alpha & 1-4T & -\beta & & \\ & & \ddots & \ddots & \ddots & \\ -\beta & & & & & \end{pmatrix}.$$

This matrix D is cyclic (that is, $D_{\nu\mu}$ depends only on $\nu-\mu$) reflecting the cyclic condition of the patterns $x^{\nu+p}=x^{\nu}$. The eigenvalue of D can be easily calculated and its largest value is

$$\lambda_{\max}=\frac{\alpha-\beta+1-4T}{4T}. \tag{4.4}$$

The solution $\delta^{\nu}=d$ is stable when the largest eigenvalue $\lambda_{\max}$ is negative. This stability of $\delta^{\nu}=d$ ceases at $T_0=(\alpha-\beta+1)/4$, where the deviation d itself also diverges. Actually, the present high-temperature expansion breaks down at a higher temperature than $T_0=(\alpha-\beta+1)/4$ (see figure 4). Therefore it is not appropriate to regard this T_0 as a critical temperature between the paramagnetic phase at high temperatures and the limit cycle phase at low temperatures. The limit cycle solution emerges as a result of complex cooperation of x^{ν}'s and the behaviour of the network has strong dependence on the initial condition. Recall that all the arguments in this paper are restricted to the case with the initial condition $\boldsymbol{x}=(1,0,0,\ldots,0)$. For example, when $\alpha=0.8$, $\beta=0.8$ and $U=0.5$ at $T=0$, if started from $(1,0,0,\ldots,0)$, the limit cycle can exist (see (3.9) ~ (3.11)). However, if started from $(0,0,\ldots,0)$, the network does not evolve with time since $(0,0,\ldots,0)$ is a stable fixed point at $T=0$. The critical temperature cannot be calculated by the present expansion analysis. We exploit the numerical method to

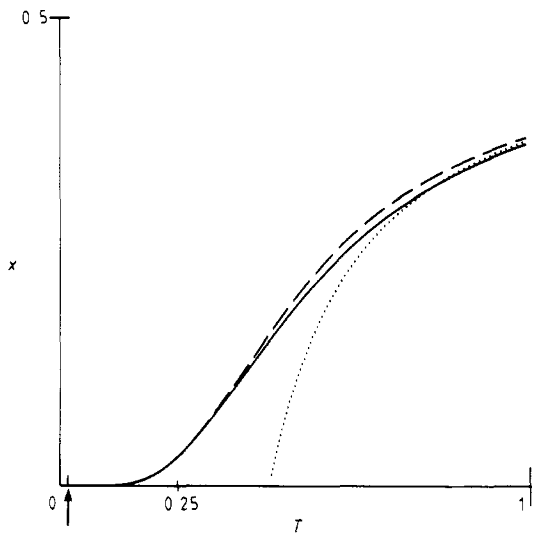

Figure 4. Fixed point values obtained by (i) the high temperature expansion (dotted line), (ii) the $x\cong 0$ expansion (broken curve) and (iii) the numerical computation (full curve) for $\alpha=0.9$, $\beta=0.9$ and $U=0.89$. The transition temperature is $T_c\cong 0.017$ (arrow).

estimate T_c as a function of the parameters in section 5. The rest of this section is dedicated to the estimation of the value of the fixed point solution.

4.2. Expansion near $x = 0$ and $x = 1$

Numerical solutions of (2.5) with $\alpha = 0.8$, $\beta = 0.8$ and $U = 0.8$ at $T = 0.01$ and 0.5 are shown in figure 5. We solved this coupled equation by the Runge-Kutta method with a time step $dt = 0.05$. It is seen that the overlaps, x^ν's, all converge to the same value close to zero at temperatures above a critical temperature $T_c = 0.017$ if started from a single pattern retrieval state $\boldsymbol{x} = (1, 0, \ldots, 0)$. x^ν's could tend to the value close to 1 (see figure 6) for other parameter sets. In the paramagnetic phase ($T > T_c$), the fixed point value approaches $\frac{1}{2}$, which is the fixed point value at $T = \infty$, with the increase of the temperature. In this phase the overlap value coincides with the activity of the network because of the randomness of firing neurons; each neuron is firing with probability x above T_c.

For the estimation of the fixed point value of x at intermediate temperatures, we solve the following fixed point equation derived from (2.5)

$$x = \frac{1}{1 + \exp[-\{(\alpha - \beta + 1)x - U\}/T]} \tag{4.5}$$

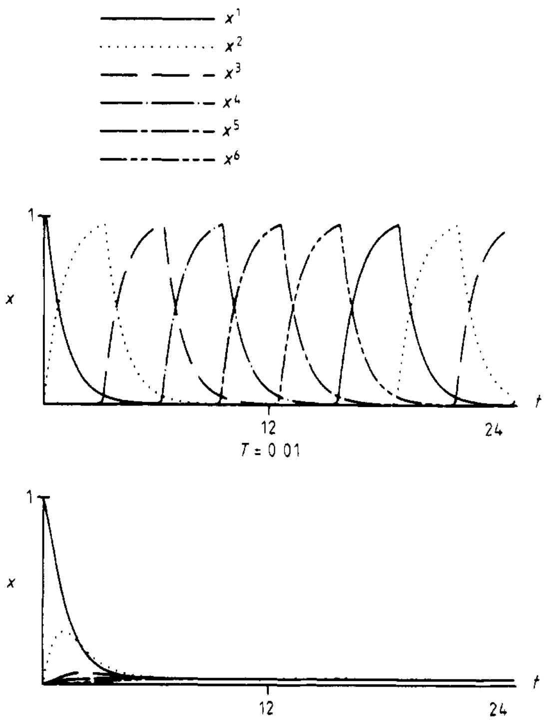

Figure 5. Numerical solution of the evolution equation (2.5) in the low-temperature phase (the upper diagram) and in the high-temperature phase (the lower one) with a Range-Kutta step, $dt = 0.06$. $\alpha = 0.9$, $\beta = 0.9$, $U = 0.89$.

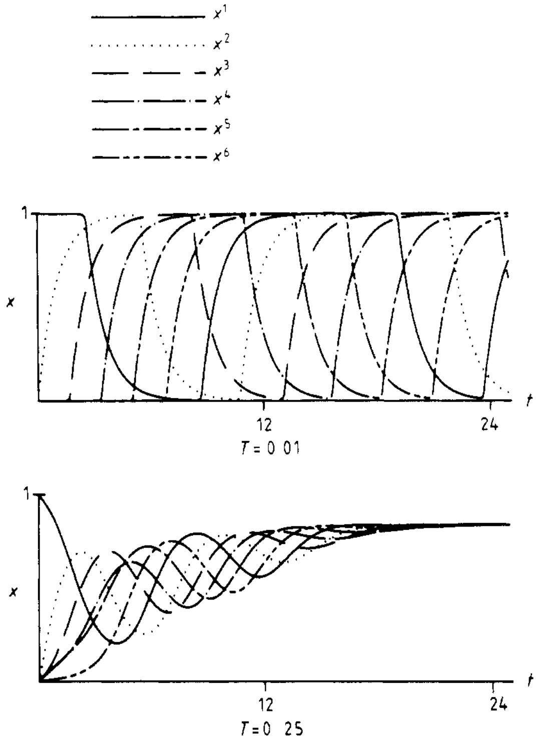

Figure 6. Same as figure 4 with different parameter sets: $\alpha = 0.6$, $\beta = 0.5$, $U = 0.51$.

in the neighbourhood of $x = 1$ or $x = 0$. Here, we have assumed that x^ν is independent of ν. A solution of the above equation is stable if the derivative of the RHS at that point is smaller than 1. As the RHS of (4.5) is a sigmoidal function, the derivative of the RHS is small if $x \neq U/(\alpha - \beta + 1)$. We expand the RHS of the equation to first order near $x = 0$, 1 and solve the resulting equation to find

$$x = \begin{cases} \dfrac{-(1+a)T}{a(\alpha-\beta+1)-(1+a)^2 T} & \text{with } a = \exp[U/T] \qquad (x \simeq 0) \\[2ex] \dfrac{b(\alpha-\beta+1)-(1+b)T}{b(\alpha-\beta+1)-(1+b)^2 T} & \text{with } b = \exp[-(\alpha-\beta+1-U)/T] \qquad (x \simeq 1). \end{cases} \tag{4.6}$$

If the threshold U is near 0, a neuron fires easily, which leads to the rather large activity. Correspondingly the fixed point assumes the lower expression of (4.6). If U is close to 1, the upper expression of (4.6) can be stable because it is not easy for neurons to fire with large U, and as a result the overlap as well as the activity does not have a large value. If U is around 0.5 and $\alpha \approx \beta$, the final fixed point is determined by the initial condition, and both points ($x \simeq 0$ and 1) of (4.6) are stable in its neighbourhood.

We have checked this argument by numerically solving (2.5). Figure 4 shows good agreement of the high-temperature expansion with the numerical results in the high-temperature region ($T \geqslant 1$). In the lower-temperature side, the expansion near $x \simeq 0$ proves to be a good approximation until the limit cycle solution appears.

5. Transition temperature

We numerically solved the evolution equation (2.5) to estimate the transition temperature. The resulting phase diagram is given in figure 7(*a*). The paramagnetic phase (FP) is separated from the limit cycle phase (LC) by the boundary drawn in figure 7(*a*).

If we fix the parameter set (α, β, U) at a value which generates a limit cycle at $T=0$ and increase T from 0 (the dashed line in figure 7(*a*)), the network suddenly changes its phase at T_c, like a first-order phase transition. In other words, the amplitude of the limit cycle jumps from a finite value to zero there. A paramagnetic fixed point is stable above T_c. It is possible to interpret the phase transition at T_c in the following words. At finite temperatures the trajectory of the network in the overlap space does not change abruptly at a boundary hyperplane of subdomains in contrast to the $T=0$ case explained in section 3. This behaviour may be expressed as a softening of the boundary. As a result the basin of attraction of the origin $(0, 0)$ gradually penetrates out from that at $T=0$. This basin of attraction eventually reaches the limit cycle trajectory, which is also diminishing with the increase of T, leading to the collapse of a limit cycle. This is the typical behaviour of a network at finite temperature which satisfies the limit cycle condition at $T=0$.

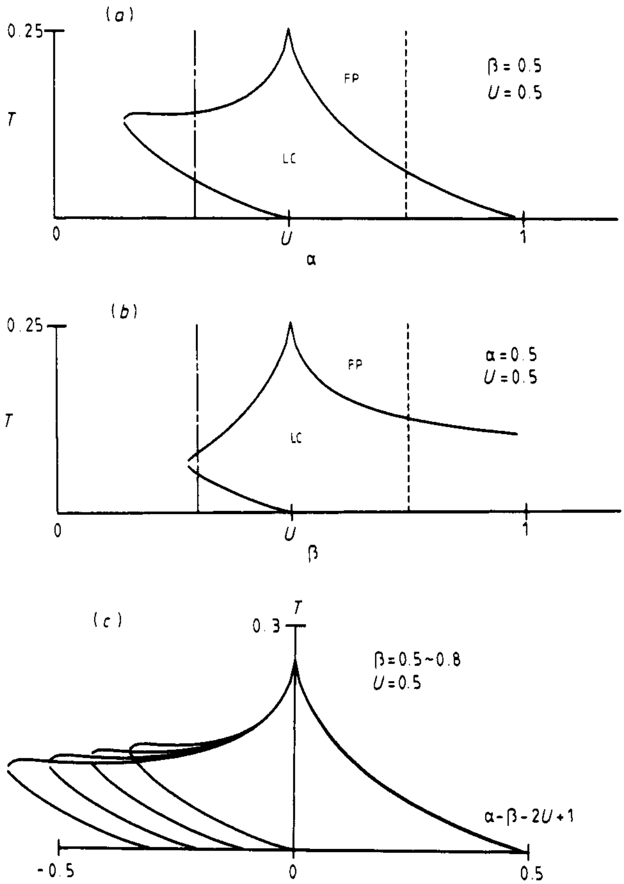

Figure 7. Phase diagram obtained by numerically solving the evolution equation. The abscissa is α in (*a*) β in (*b*) and $\alpha-\beta-2U+1$ in (*c*).

When the parameters are chosen such that the system falls into a fixed point at $T=0$ (the dash-dot line in figure 7(a)), the situation is a little different. Such a network could sometimes have a limit cycle solution at $T>0$. This may seem quite a different phenomenon from the previous case of collapse of a limit cycle with the increase of temperature. However, the qualitative argument given above applies without major modifications. It is seen in figure 8 that $(1,1)$ is a stable fixed point at $T=0$ with the parameters which do not satisfy the limit cycle condition at $T=0$. At finite temperatures the boundary wall becomes obscure, and the flow vector (tangential vector of the trajectory) begins to cross the $T=0$ boundary wall leading to a limit cycle. This behaviour has been observed by Buhmann and Schulten. They thus concluded that the system has a limit cycle solution only at $T>0$. We have shown that an appropriate set of parameters (α, β, U) yields a limit cycle even at $T=0$.

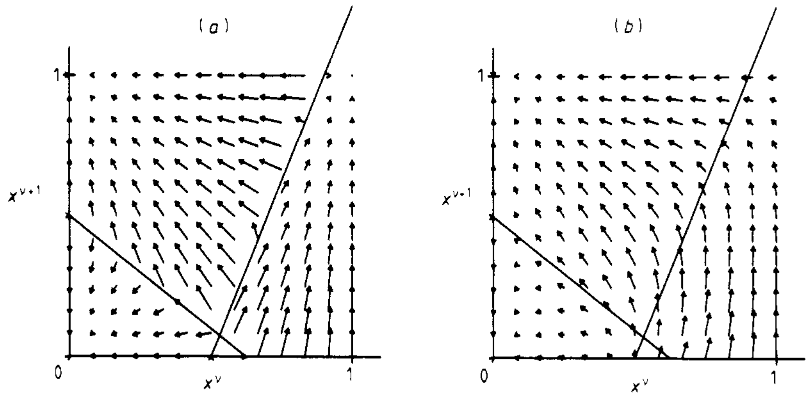

Figure 8. Flow vectors on the $(x^{\nu}, x^{\nu+1})$ plane for $\alpha=0.8$, $\beta=0.4$, $U=0.5$ at (a) $T=0$ and (b) $T=0.1$.

The phase boundaries in figure 7(a) approximately coincide in the range $\alpha-\beta-2U+1>0$ if we plot the diagram with the abscissa $\alpha-\beta-2U+1$ for a fixed value of the threshold U (see figure 7(c)), except for the re-entrance boundary line above which the limit cycle solution can exist (see figure 6(a)). Although a different U gives a different diagram, α and β do not determine the transition temperature independently. We first explain the shape of the phase boundary of the higher-temperature side in figure 7(a) qualitatively and then derive the re-entrance boundary line analytically.

The boundary is seen to have a peak at $\alpha-\beta-2U+1=0$ for most parameter sets. This numerical result may be explained qualitatively as follows. When $\alpha-\beta-2U+1=0$ is satisfied, the flow vector is antisymmetric under the transformation,

$$x^{\nu} \to 1-x' \qquad (\nu=1,\ldots,p) \tag{5.1}$$

in the p-dimensional phase space of the overlap as is seen in the following relation.

$$\dot{x}^{\nu} = -x^{\nu} + \frac{1}{1+\exp[-(\alpha x^{\nu-1}+x^{\nu}-\beta x^{\nu+1}-U)/T]} \to -\dot{x}^{\nu}. \tag{5.2}$$

This antisymmetry implies that the basin of attraction of the origin always has the same shape as that of the other stable fixed point $(1,1,\ldots,1)$. These two basins of attraction penetrate out simultaneously with the increase of temperature from both ends of the phase space. If a limit cycle trajectory stays as far as possible from

$(0, 0, \ldots, 0)$ and $(1, 1, \ldots, 1)$, the trajectory does not collapse easily by the penetration of the two basins of attraction. In other words, the transition temperature is high if the trajectory is on or near the hyperplane

$$x^1 + x^2 + \ldots + x^p = \frac{p}{2} \tag{5.3}$$

which is the bisector of the line connecting $(0, 0, \ldots, 0)$ and $(1, 1, \ldots, 1)$. It has been verified numerically that the limit cycle trajectory approximately stays on the plane (5.3) for various parameters satisfying $\alpha - \beta - 2U + 1 = 0$ at any temperature. It is also remarked that any limit cycle trajectory stays on or near some hyperplane, $x_{\text{sum}} = x^1 + x^2 + \ldots + x^p = \text{constant}$, as seen in figure 9; the evolution equation of x_{sum} can be written as

$$\dot{x}_{\text{sum}} = -x_{\text{sum}} + \sum_{\nu} \frac{1}{1 + \exp[-(\alpha x^{\nu-1} + x^{\nu} - \beta x^{\nu+1} - U)/T]}. \tag{5.4}$$

After some transient period the second term on the RHS becomes a periodic function of time from the cyclic permutation invariance of the indices (see figure 9). Thus x_{sum} oscillates around the value determined approximately by $\dot{x}_{\text{sum}} = 0$.

The re-entrance boundary lines are derived as follows. We first discuss the case of figure 7(a) whose abscissa is α. For $\alpha < U$, a limit cycle cannot exist at $T = 0$ since the fixed point $\boldsymbol{x} = (1, 0, \ldots, 0)$ becomes stable. At finite temperatures the penetration of the attraction basin of $(x^{\nu}, x^{\nu+1}) = (1, 1)$ on the $(x^{\nu}, x^{\nu+1})$-plane capture the fixed point near $(1, 0)$. Thus the limit cycle exists above some temperature. The penetrated

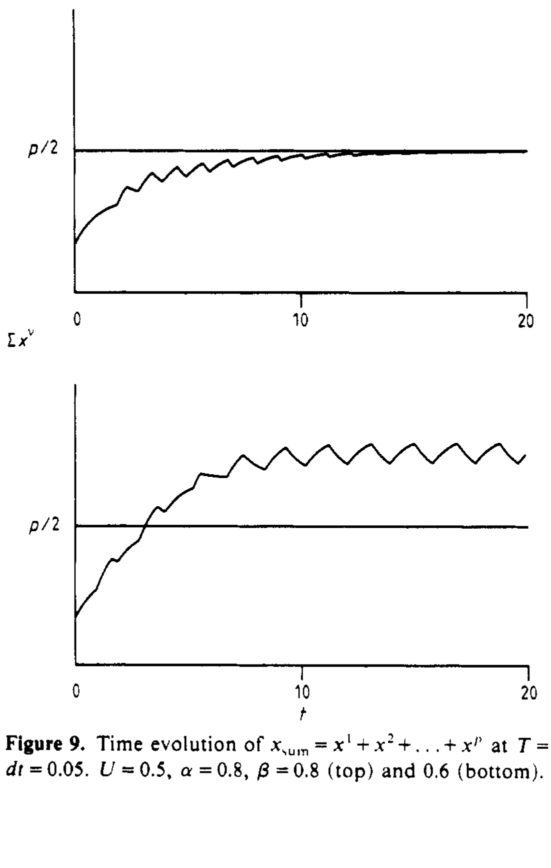

Figure 9. Time evolution of $x_{\text{sum}} = x^1 + x^2 + \ldots + x^p$ at $T = 0.01$ with a Runge–Kutta step, $dt = 0.05$. $U = 0.5$, $\alpha = 0.8$, $\beta = 0.8$ (top) and 0.6 (bottom).

boundary line is given by a limiting procedure as follows. The flow vector on the $(x^\nu, x^{\nu+1})$ plane is

$$\begin{pmatrix} \dot{x}^\nu \\ \dot{x}^{\nu+1} \end{pmatrix} = \begin{pmatrix} -x^\nu + 1/\{1+\exp[-y^\nu/T]\} \\ -x^{\nu+1} + 1/\{1+\exp[-y^{\nu+1}/T]\} \end{pmatrix} \tag{5.5}$$

where

$$\begin{aligned} y^\nu &= \alpha x^{\nu-1} + x^\nu - \beta x^{\nu+1} - U \\ y^{\nu+1} &= \alpha x^\nu + x^{\nu+1} - \beta x^{\nu+2} - U. \end{aligned} \tag{5.6}$$

The meaning of y^ν is the horizontal distance from one of the $T=0$ boundary lines, and $y^{\nu+1}$ is the vertical distance from the other boundary line as shown in figure 10. If the flow vector $\boldsymbol{A}$ at $\boldsymbol{P}$ in figure 10 points to a target located across the $T=0$ boundary line, this point $\boldsymbol{P}$ is included in the penetration of the attraction basin of (1, 1), because in this case the phase point moves toward the $T=0$ boundary line until it eventually reaches there. The flow vector heads for a point across the $T=0$ boundary line, if

$$[\boldsymbol{A}\times\boldsymbol{B}]_z < 0 \tag{5.7}$$

where $\boldsymbol{A}$ is the flow vector and $\boldsymbol{B}$ is a vector directed toward $(1, U-\alpha)$

$$\boldsymbol{A} = \begin{pmatrix} \dot{x}^\nu \\ \dot{x}^{\nu+1} \end{pmatrix}$$

$$\boldsymbol{B} = \begin{pmatrix} -x^\nu + 1 \\ -x^{\nu+1} + (U-\alpha) \end{pmatrix}.$$

In other words, if $\boldsymbol{A}$ points to somewhere above $\boldsymbol{B}$, the third component of the vector product $\boldsymbol{A}\times\boldsymbol{B}$ is negative (see figure 10). We could set the components other than x^ν and $x^{\nu+1}$ zero here. We restrict ourselves to the case $y^\nu \gg T$, that is, the νth component of the target point is always 1 and $\dot{x}^\nu = -x^\nu + 1$ (see (5.5)). Equation (5.7) can then be written as

$$y^{\nu+1} > T \ln \frac{U-\alpha}{1-(U-\alpha)}. \tag{5.8}$$

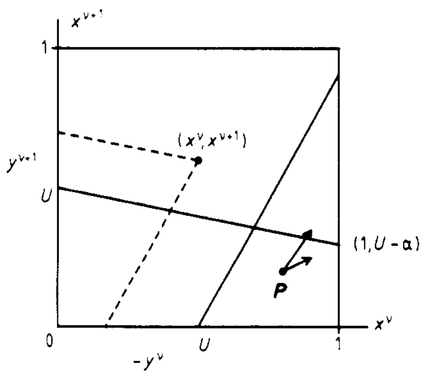

Figure 10. Phase plane $(x^\nu, x^{\nu+1})$ for the estimation of the re-entrance transition temperature. y^ν and $y^{\nu+1}$ correspond to the horizontal and the vertical distances from the corresponding boundary lines at $T=0$ as shown in the figure for a given $(x^\nu, x^{\nu+1})$. $\alpha=0.2$, $\beta=0.55$, $U=0.5$.

We draw a line satisfying $y^{\nu+1} = T\ln[(U-\alpha)/(1-U+\alpha)]$ parallel to the $T=0$ boundary line. We call this line the first penetration boundary line. This first penetration boundary line crosses $x^\nu = 1$ at

$$(x^\nu, x^{\nu+1}) = \left(1,\ T\ln\frac{U-\alpha}{1-(U-\alpha)} + U - \alpha\right) \equiv (1, a_1). \tag{5.9}$$

Estimation of the penetration is not complete yet. There are some flow vectors which cross the above first boundary line denoted by a_1 of (5.9). The second boundary line is given in the same manner as above with replacement $(U-\alpha) \to T\ln[(U-\alpha)/\{1-(U-\alpha)\}] + U - \alpha = a_1$. This second boundary line is parallel to that of the first and has the point $(1, a_2)$ on it where a_2 is

$$\begin{aligned} a_1 &= T\ln\frac{U-\alpha}{1-(U-\alpha)} + U - \alpha \\ a_2 &= T\ln\frac{a_1}{1-a_1} + U - \alpha. \end{aligned} \tag{5.10}$$

There are also some flow vectors crossing this second boundary line. These vectors form the third boundary line given by $a_3 = T\ln[a_2/(1-a_2)] + U - \alpha$. In general, the nth boundary line is parallel to the $T=0$ boundary line and has the point $(1, a_n)$ on it with a_n given by the recursion relation

$$\begin{aligned} a_0 &= U - \alpha \\ a_{n+1} &= T\ln\frac{a_n}{1-a_n} + U - \alpha. \end{aligned} \tag{5.11}$$

If the sequence $\{a_n\}$ converges to the limit $0 < a_\infty < 1$, the penetrated boundary line of attraction basin of $(x^\nu, x^{\nu+1}) = (1, 1)$ at finite T exists; that is, when the following equation has a solution in the range $0 < a_\infty < 1$.

$$a_\infty = T\ln\frac{a_\infty}{1-a_\infty} + U - \alpha. \tag{5.12}$$

On the other hand, a fixed point near $(x^\nu, x^{\nu+1}) = (1, 0)$ at a finite temperature satisfies

$$\begin{aligned} \dot{x}^\nu &= 0 = -x^\nu + \frac{1}{1+\exp[-y^\nu/T]} \\ \dot{x}^{\nu+1} &= 0 = -x^{\nu+1} + \frac{1}{1+\exp[-y^{\nu+1}/T]}. \end{aligned} \tag{5.13}$$

Using the approximation $y^\nu \gg T$, we have $x^\nu = 1$ and

$$x^{\nu+1} = \frac{1}{1+\exp[-\{x^{\nu+1} - (U-\alpha)\}/T]}. \tag{5.14}$$

Capture of this stable fixed point by the penetrated attraction basin occurs when

$$x^{\nu+1} > a_\infty \tag{5.15}$$

with $x^{\nu+1}$ and a_∞ given by (5.12) and (5.14). Therefore, T_c is obtained by the condition $x^{\nu+1} = a_\infty$. It is easily seen that (5.12) is the inverse function of (5.14). The solutions a_∞ and $x^{\nu+1}$ are given as a cross point of $y = 1/\{1+\exp[-\{x-(U-\alpha)/T\}]\}$ and $y = x$. This sigmoidal function touches $y = x$ at $x_c > 0$ at the transition temperature. We have found that the result of this argument agrees with the numerical T_c within 0.1% errors for various parameter sets. This agreement implies validity of our picture of transition from the fixed point phase to the limit cycle phase. The re-entrance transition temperatures of figure 7(*b*), whose abscissa is β, can be obtained in the same manner as above with simple replacement $(U-\alpha) \to (\beta + U)$. The result agrees again with numerical estimates within 0.1% errors.

6. Summary and discussion

For a neural network originally formulated by Buhmann and Schulten, we deduced limit cycle conditions at $T=0$ from a stability analysis on the phase plane. It has been possible to treat the system analytically at $T=0$ as the phase space is divided by p hyperplanes into 2^p subdomains in each of which the system evolves along a straight trajectory. These limit cycle conditions are expressed as restrictions on the parameter set (α, β, U) (equations (3.9)-(3.11)) and the value of x^ν's (equations (3.6) and (3.7)). We restricted the initial condition to a single-retrieval state $\boldsymbol{x}=(1,0,0,\ldots,0)$. The behaviours of the system at higher temperatures were investigated, and the high-temperature fixed point solution is obtained approximately (equation (4.3)). Transition temperatures between the fixed point phase and the limit cycle phase were calculated numerically. Weak dependency on α and β and stronger dependency on U of transition temperatures are observed. Phase diagrams are observed to be scaled with $\alpha-\beta-2U+1$. The phase boundaries have a peak at $\alpha-\beta-2U+1=0$. For $\alpha-\beta-2U+1=0$, the phase space is antisymmetric under the transformation, $x^\nu \to 1-x^\nu$, and the limit cycle trajectory stays away from the two attractive fixed points $(0,0,\ldots,0)$ and $(1,1,\ldots,1)$. A re-entrance boundary line between a fixed point phase at lower temperatures and a limit cycle phase at intermediate temperatures is derived analytically. Analytically derived T_c agrees with numerical result within 0.1% errors.

For the estimation of a transition temperature between a limit cycle phase and a paramagnetic fixed point phase at higher temperatures, we cannot use the approximations which we applied for the estimation of the re-entrance transition temperature. The reason is that the components of the overlap vector other than x^ν and $x^{\nu+1}$ have finite values which we set zero in the latter case. This implies the discussion on the phase plane $(x^\nu, x^{\nu+1})$ does not work in estimation of the transition temperature. That is a main reason we could not derive the boundary line of the higher-temperature side analytically.

References

Amari S 1972 *IEEE Trans. Comput.* **C-21** 1197-1206
Buhmann J and Schulten K 1987 *Europhys. Lett.* **4** 1205-9
Hopfield J J 1982 *Proc. Natl Acad. Sci. USA* **79** 2554-8
Nishimori H, Nakamura T and Shiino M 1990 *Phys. Rev.* A **41** 3346-54
Sompolinsky H and Kanter I 1986 *Phys. Rev. Lett.* **57** 2861-4